The density matrix renormalization group for a quantum spin chain at non-zero temperature

LETTER TO THE EDITOR

The density matrix renormalization group for a quantum spin chain at non-zero temperature

R J Bursill†§, T Xiang‡ and G A Gehring†

† Department of Physics, The University of Sheffield, Sheffield S3 7RH, UK
‡ Interdisciplinary Research Centre in Superconductivity, The University of Cambridge, Cambridge CB3 0HE, UK

Abstract. We apply a recent adaptation of White's density matrix renormalization group (DMRG) method to a simple quantum spin model, the dimerized XY chain, in order to assess the applicability of the DMRG to quantum systems at non-zero temperature. We find that very reasonable results can be obtained for the thermodynamic functions down to low temperatures using a very small basis set. Low-temperature results are found to be most accurate in the case when there is a substantial energy gap.

Since its recent inception, White's density matrix renormalization group (DMRG) method has been established as the method of choice for determining static, low-energy properties of one-dimensional quantum lattice systems [1, 2]. Extensions to the calculation of dynamical properties [3] and even to the study of low-temperature properties of two-dimensional systems [4] have been forthcoming. Moreover, Nishino's formulation of the DMRG for two-dimensional classical systems [5] has paved the way for the study of one-dimensional quantum systems at non-zero temperature. In this letter we present what is, to the best of our knowledge, the first application of the DMRG to the thermodynamics of a quantum system.

The system that we consider is a simple spin-chain model—the dimerized, $S = 1/2$, XY model

$$\mathcal{H} = -\sum_{i=1}^{N/2} \left[J_1(S_{2i-1}^x S_{2i}^x + S_{2i-1}^y S_{2i}^y) + J_2(S_{2i}^x S_{2i+1}^x + S_{2i}^y S_{2i+1}^y) \right] \tag{1}$$

where S_i is a spin-1/2 operator for site i on an (even) chain of N sites, with periodic boundary conditions.

This model is exactly solvable [6]; the Helmholtz free energy ψ is given by

$$-\beta\psi = \lim_{N\to\infty} \frac{\log Z_N}{N} = \frac{1}{2\pi} \int_0^{2\pi} \log\left[2\cosh\frac{\beta\phi(\theta)}{4} \right] d\theta \tag{2}$$

where $Z_N = \text{Tr } e^{-\beta\mathcal{H}}$ is the partition function, $\beta \equiv 1/T$ is the inverse temperature, $\phi(\theta) = \cos\xi(\theta) + \gamma\cos(\theta + \xi(\theta))$, $\gamma \equiv J_2/J_1$,

$$\xi(\theta) = -\tan^{-1}\frac{\gamma\sin\theta}{1 + \gamma\cos\theta}$$

§ Present address: School of Physics, UNSW, Sydney, 2052, Australia.

and we have set $J_1 = 1$. Thermodynamic properties such as the internal energy

$$u = -\frac{\partial \beta \psi}{\partial \beta}$$

and the specific heat $c_V = -\beta^2 \, \partial u / \partial \beta$ are readily obtainable from equation (2).

Because of its solvability and the fact that it possesses both gapless ($\gamma = 1$) and gapped ($\gamma \neq 1$) excitations, equation (1) presents a useful test model for the extension of the DMRG to quantum systems at non-zero temperature.

Now Nishino's formulation of the DMRG applies directly to classical, two-dimensional spin systems and so in order to apply it to the quantum system (1), we must first invoke the Trotter–Suzuki method [7]. That is, we make the decomposition $\mathcal{H} = \mathcal{H}_1 + \mathcal{H}_2$ where

$$\mathcal{H}_1 = -J_1 \sum_{i=1}^{N/2} h_{2i-1,2i} \qquad \mathcal{H}_2 = -J_2 \sum_{i=1}^{N/2} h_{2i,2i+1} \tag{3}$$

and $h_{i,j} \equiv S_i^x S_j^x + S_i^y S_j^y$. We then apply the formula

$$Z_N = \lim_{M\to\infty} Z_{MN} \equiv \lim_{M\to\infty} \mathrm{Tr}\left[\mathrm{e}^{-\beta\mathcal{H}_1/M}\mathrm{e}^{-\beta\mathcal{H}_2/M}\right]^M . \tag{4}$$

Inserting a collection σ of $2M$ complete sets of states into (4) then yields

$$Z_{MN} = \sum_{\sigma}\prod_{j=1}^{M} \langle \sigma_1^{2j-1}\cdots\sigma_N^{2j-1}|\mathrm{e}^{-\beta\mathcal{H}_1/M}|\sigma_1^{2j}\cdots\sigma_N^{2j}\rangle$$

$$\times \langle \sigma_1^{2j}\cdots\sigma_N^{2j}|\mathrm{e}^{-\beta\mathcal{H}_2/M}|\sigma_1^{2j+1}\cdots\sigma_N^{2j+1}\rangle \tag{5}$$

where periodic boundary conditions $\sigma_i^{2M+1} \equiv \sigma_i^1$, $\sigma_{N+1}^j \equiv \sigma_1^j$ are assumed.
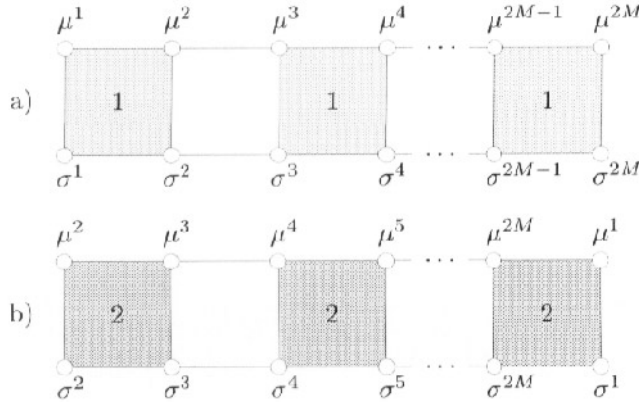

Figure 1. A pictorial representation of the matrices (a) $\mathcal{T}_1(\mu^1\cdots\mu^{2M}|\sigma^1\cdots\sigma^{2M})$ and (b) $\mathcal{T}_2(\mu^1\cdots\mu^{2M}|\sigma^1\cdots\sigma^{2M})$.

Now, because the $N/2$ terms in the sums (3) commute and act on different pairs of sites, we have

$$Z_{MN} = \sum_{\sigma}\prod_{i=1}^{N/2}\prod_{j=1}^{M} \tau_1(\sigma_{2i-1}^{2j-1}\sigma_{2i}^{2j-1}|\sigma_{2i-1}^{2j}\sigma_{2i}^{2j})\tau_2(\sigma_{2i}^{2j}\sigma_{2i+1}^{2j}|\sigma_{2i}^{2j+1}\sigma_{2i+1}^{2j+1}) \tag{6}$$
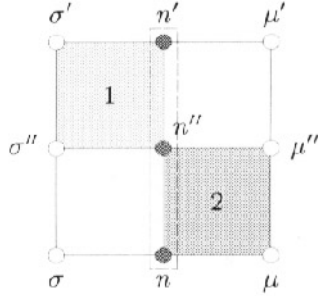
Figure 2. A pictorial representation of the initial system block transfer matrix $T_s(\sigma'n'\mu'|\sigma n\mu; \sigma''\mu'')$. n and $n' = 1, \ldots, m = 2$ are initial and final states of the system block which consists of a single site. σ, σ'' and $\sigma' = \uparrow$ or $\downarrow$ and μ, μ'' and $\mu' = \uparrow$ or $\downarrow$ are initial, intermediate and final states for the adjacent sites to the left and right of the block respectively. The intermediate state n'' of the system block is summed over to produce the matrix product.

where

$$\tau_i(\sigma'\mu'|\sigma\mu) \equiv \langle\sigma'\mu'|e^{\beta J_i h_{1,2}/M}|\sigma\mu\rangle \tag{7}$$

for $i = 1, 2$. Moreover,

$$Z_{MN} = \sum_\sigma \prod_{i=1}^{N/2} T_1(\sigma_{2i-1}^1 \ldots \sigma_{2i-1}^{2M}|\sigma_{2i}^1 \ldots \sigma_{2i}^{2M}) T_2(\sigma_{2i}^1 \ldots \sigma_{2i}^{2M}|\sigma_{2i+1}^1 \ldots \sigma_{2i+1}^{2M}) \tag{8}$$

or

$$Z_{MN} = \operatorname{Tr} T^{N/2} \tag{9}$$

where $T \equiv T_1 T_2$ is the *virtual transfer matrix* and

$$T_1(\mu^1 \ldots \mu^{2M}|\sigma^1 \ldots \sigma^{2M}) \equiv \prod_{j=1}^M \tau_1(\mu^{2j-1}\sigma^{2j-1}|\mu^{2j}\sigma^{2j}) \tag{10}$$

$$T_2(\mu^1 \ldots \mu^{2M}|\sigma^1 \ldots \sigma^{2M}) \equiv \prod_{j=1}^M \tau_2(\mu^{2j}\sigma^{2j}|\mu^{2j+1}\sigma^{2j+1}). \tag{11}$$

The matrices T_1 and T_2 are depicted graphically in figure 1.

It follows [7] that

$$\psi = \psi^{(M)} \equiv \lim_{M \to \infty} -\frac{\log \lambda_{\max}}{2\beta} \tag{12}$$

where $\lambda_{\max}$ is the eigenvalue of T with maximal modulus and generally depends on the Trotter dimension M.

We may now apply the formulation of the DMRG for transfer matrices to the calculation of $\lambda_{\max}$. We commence by defining an initial transfer matrix T_s for a single-site *system block*, which connects it to adjacent sites to the left and the right, namely

$$T_s(\sigma'n'\mu'|\sigma n\mu; \sigma''\mu'') = \sum_{n''} \tau_1(\sigma'\sigma''|n'n'')\tau_2(n''n|\mu''\mu). \tag{13}$$

The initial block, having just one site, has $m = 2$ states, $n = 1$ or 2 ($\uparrow$ or $\downarrow$) (see figure 2).

We next define an initial *environment block* and associated transfer matrix T_e in precisely the same way: $T_e \equiv T_s$. We define a *superblock* using the system and environment blocks
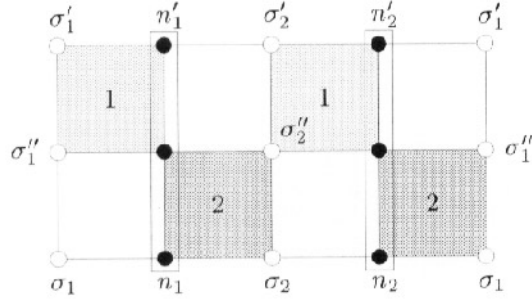
Figure 3. A pictorial representation of the superblock, which consists of system and environment blocks connected by two added sites to form a periodic chain. n_1 and n_1' and n_2 and n_2' are initial- and final-state indices for the system and environment blocks respectively. σ_1 and σ_1' and σ_2 and σ_2' are initial and final states for the two added sites. The intermediate states σ_1'' and σ_2'' are summed over to form the matrix product.

in addition to two added sites, arranged in a periodic fashion (see figure 3). That is, the superblock transfer matrix is given by

$$\mathcal{T}(\sigma_1'n_1'\sigma_2'n_2'|\sigma_1 n_1 \sigma_2 n_2) = (\mathcal{T}_1\mathcal{T}_2)(\sigma_1'n_1'\sigma_2'n_2'|\sigma_1 n_1 \sigma_2 n_2) \tag{14}$$

or

$$\mathcal{T}(\sigma_1'n_1'\sigma_2'n_2'|\sigma_1 n_1 \sigma_2 n_2) = \sum_{\sigma_1''\sigma_2''} \mathcal{T}_s(\sigma_1'n_1'\sigma_2'|\sigma_1 n_1 \sigma_2; \sigma_1''\sigma_2'')\mathcal{T}_e(\sigma_2'n_2'\sigma_1'|\sigma_2 n_2 \sigma_1; \sigma_2''\sigma_1''). \tag{15}$$

At this point $\mathcal{T}$ may be diagonalized to determine $\lambda_{\max}$ and hence the $M = 2$ approximation (12) to (2).

In order to proceed to larger lattices, we must augment (expand) the system and environment blocks. We let $n \longleftrightarrow (p, \nu)$, $p = 1, \ldots, m$, $\nu = \uparrow, \downarrow$ denote a state for an augmented-system block, consisting of the initial system block and one site added to the right. There are now $m' = 2m = 4$ states: $n = 1 \longleftrightarrow (1, \uparrow), \ldots, n = 4 \longleftrightarrow (2, \downarrow)$.

The transfer matrix $\mathcal{T}_s'$ for the augmented-system block is defined (see figure 4) by

$$\mathcal{T}_s'(\sigma'n'\mu'|\sigma n \mu; \sigma''\mu'') \equiv \sum_{\nu''} \mathcal{T}_s(\sigma'p'\nu'|\sigma p \nu; \sigma''\nu'')\tau_1(\nu'\nu''|\mu'\mu''). \tag{16}$$

An augmented-environment block is defined in a similar way, this time adding a site to the left, namely

$$\mathcal{T}_e'(\sigma'n'\mu'|\sigma n \mu; \sigma''\mu'') \equiv \sum_{\nu''} \mathcal{T}_e(\sigma'p'\nu'|\sigma p \nu; \sigma''\nu'')\tau_2(\sigma''\sigma|\nu''\nu). \tag{17}$$

Now, the superblock and its associated transfer matrix (15) can once again be formed using the augmented blocks with $m' \longmapsto m$, $\mathcal{T}_s' \longmapsto \mathcal{T}_s$ and $\mathcal{T}_e' \longmapsto \mathcal{T}_e$. Moreover, the process can be iterated, each time augmenting the system and environment blocks to the right and the left respectively.

However, in order to prevent the superblock basis from becoming too large, we must truncate it by capping the number of system (and environment) block states, m, which in principle doubles every iteration. To do so, we form reduced density matrices for the augmented blocks by performing an appropriate partial trace on the projection operator $|\psi_{\max}\rangle\langle\psi_{\max}|$ formed from the eigenstate $|\psi_{\max}\rangle$ of $\mathcal{T}$ corresponding to the eigenvalue $\lambda_{\max}$.
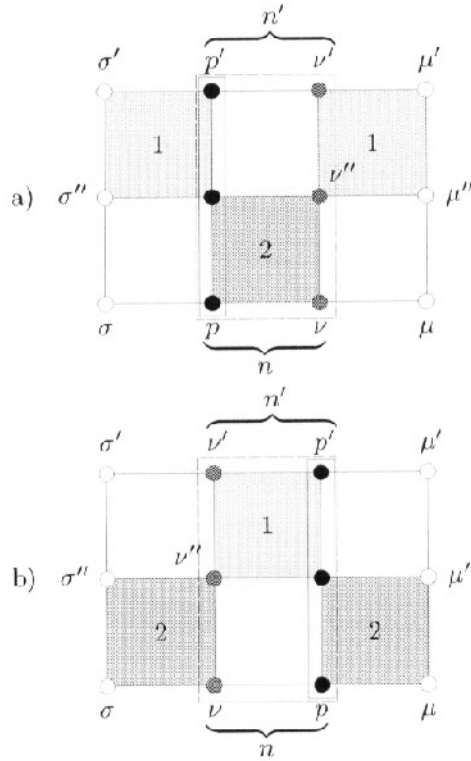
Figure 4. A pictorial representation of the (a) augmented-system and (b) augmented-environment blocks, which consist of the old blocks augmented by adding sites to the right and the left respectively. n and $n' = 1, \ldots, m'$ are the initial and final states of the new (augmented) block which consists of the old block (p and p') augmented with an added site (v and v'). σ, σ'' and σ' and μ, μ'' and μ' are state indices for the adjacent sites. The intermediate state v'' of the added site is summed over to produce the matrix product.

That is, for the augmented-system block, the density matrix ρ_s is defined by

$$\rho_s(n'|n) \equiv \sum_{\sigma_1 n_2} \langle \sigma_1 n_1' \sigma_2' n_2 | \psi_{\max} \rangle \langle \psi_{\max} | \sigma_1 n_1 \sigma_2 n_2 \rangle \tag{18}$$

where $n \longleftrightarrow (n_1, \sigma_2)$ and $n' \longleftrightarrow (n_1', \sigma_2')$. For the augmented-environment block we have

$$\rho_e(n'|n) \equiv \sum_{\sigma_1 n_1} \langle \sigma_1 n_1 \sigma_2' n_2' | \psi_{\max} \rangle \langle \psi_{\max} | \sigma_1 n_1 \sigma_2 n_2 \rangle \tag{19}$$

with $n \longleftrightarrow (n_2, \sigma_2)$ and $n' \longleftrightarrow (n_2', \sigma_2')$. Eigenvalues and eigenvectors of the density matrices are then found, namely

$$\{\omega_n^{(s)}, |n\rangle^{(s)} : n = 1, \ldots, m'\} \qquad \text{and} \qquad qs\{\omega_n^{(e)}, |n\rangle^{(e)} : n = 1, \ldots, m'\}$$

for ρ_s and ρ_e respectively where $1 \geqslant \omega_1^{(i)} \geqslant \omega_2^{(i)} \geqslant \cdots \geqslant \omega_{m'}^{(i)}$ for i = s or e.

In proceeding to the next iteration then, we represent the augmented-block transfer matrices $\mathcal{T}_s'$ and $\mathcal{T}_e'$ in terms of the density matrix eigenvectors and truncate the block Hilbert spaces so as to retain only the m most important states, namely

$$\sum_{n'', n'''=1}^{m'} \langle n'|n''\rangle^{(i)} \mathcal{T}_i'(\sigma' n'' \mu' | \sigma n''' \mu; \sigma'' \mu'')^{(i)} \langle n'''|n\rangle \longmapsto \mathcal{T}_i(\sigma' n' \mu' | \sigma n \mu; \sigma'' \mu'') \tag{20}$$
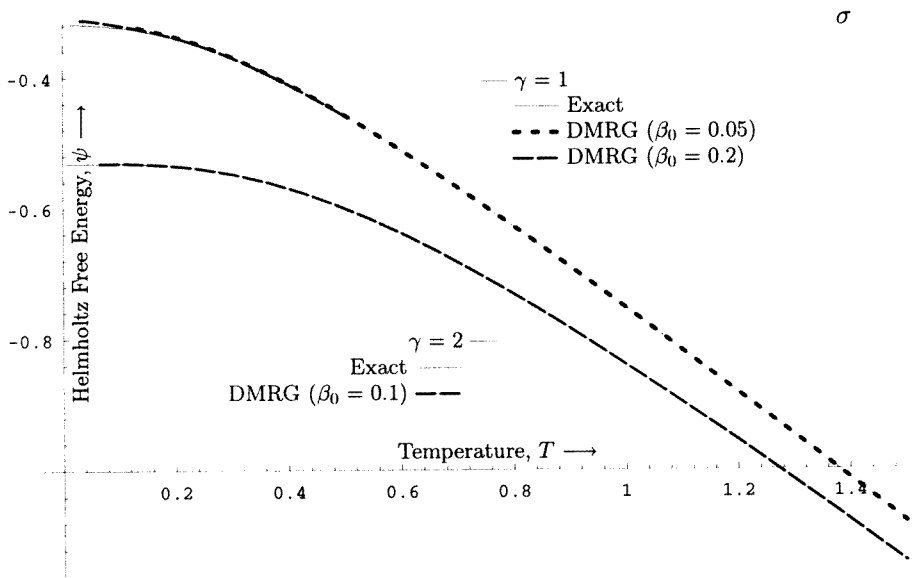
σ

Figure 5. Exact and DMRG results for the Helmholtz free energy ψ as a function of temperature T for two cases: $\gamma = 1$ and $\gamma = 2$.
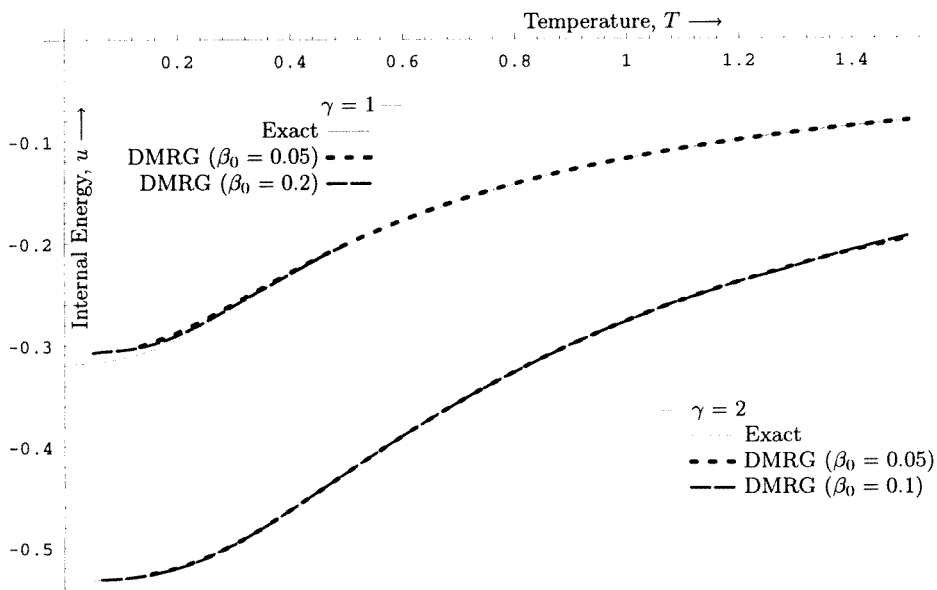

Figure 6. Exact and DMRG results for the internal energy u as a function of temperature T for two cases: $\gamma = 1$ and $\gamma = 2$.

for i = s and e, $n, n' = 1, \ldots, m$ and where m is the chosen cap on the number of states per block.

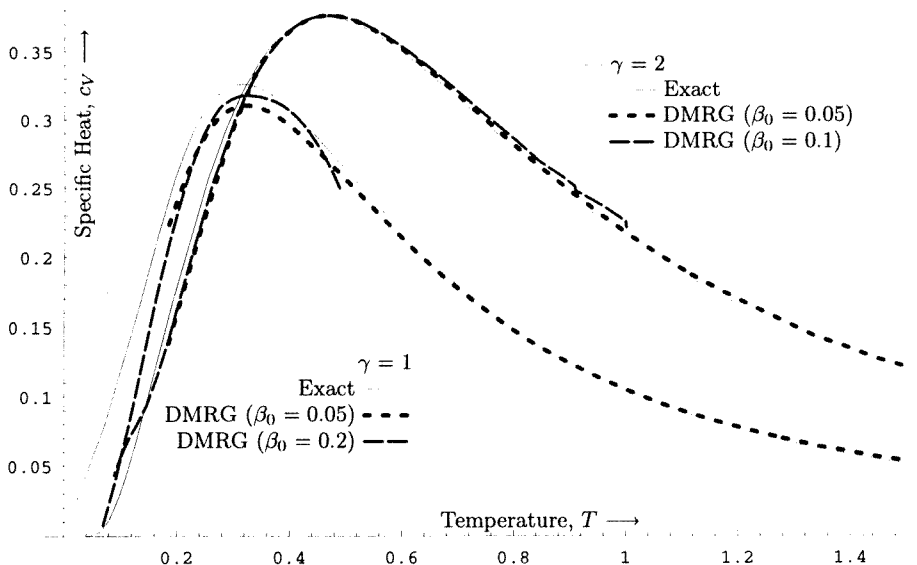Now, $\mathcal{T}$ is a large, sparse, non-symmetric matrix, for which efficient algorithms for

Figure 7. Exact and DMRG results for the specific heat c_V as a function of temperature T for two cases: $\gamma = 1$ and $\gamma = 2$.

the determination of $\lambda_{\max}$ and $|\psi_{\max}\rangle$ are becoming available. So far we have simply used Schur decomposition and the inverse power method to perform this task. We have thus only been able to work with $m = 16$. Results for ψ, u and c_V for $\gamma = 1$ (pure XY) and $\gamma = 2$ (dimerized XY) are given in figures 5–7.

Finite-M results $\psi^{(M)}$ are obtained by fixing the inverse temperature $\beta = \beta_0$ in the expressions (7) and increasing the superblock size $2M$, beginning with $M = 2$, so at each iteration the temperature is identified as $T = 1/M\beta_0$. For the β_0-values that we have considered (0.05–0.2) there is a small error due to the finiteness of the Trotter decomposition but this is negligible compared with the error due to Hilbert space truncation, a result which is easily verified by considering the exact solution for $\psi^{(M)}$ [7]. A typical calculation, using NAG library routines on a 333 MHz DEC Alpha machine, takes six hours to generate a superblock size of $2M = 300$.

We note that convergence at low temperatures is far better for the gapped system ($\gamma = 2$). However, even in the gapless case, the peak position and peak height in the specific heat are afflicted by errors of only about 3%, and results may be improved markedly by using larger values of m and the finite-lattice method [1]. Also, results for u and c_V are obtained by numerically differentiating spline fits of the computed $\psi^{(M)}$-values, and so improvements may be obtained by combining results from a number of different β_0-values.

Note that, at any given iteration, the DMRG usually works with a chain which is spatially finite. Here the chain is infinite and the finiteness is in the level of the Trotter approximation. Another difference is that the DMRG usually produces its best results for the ground-state energy and less accurate results for higher excitations. A different situation occurs here—the lower the temperature, the less accurate the result. Even so, as can be seen in figure 5, the exact ground-state energy, $\lim_{T \to 0} \psi$, is recovered with reasonable accuracy, especially in the gapped case $\gamma = 2$.

Finally, we note that, as $\mathcal{T}$ is non-symmetric, the use of a truncated basis will not in general lead to a variational lower bound on $\lambda_{\max}$. However, in practice it can be seen, for instance, that the DMRG result for the internal energy u is always bounded above the exact value.

To conclude, we have applied the DMRG to a quantum spin chain at non-zero temperature, making use of Nishimo's adaptation of the method to 2D classical systems. Reasonable results are obtained for the specific heat down to low temperatures in calculations involving an extremely small basis set, agreement with the exact solution being markedly better in the case where the system has a substantial gap. The approach may prove useful in determining thermodynamic properties of models of experimentally realizable systems such as coupled chains and models with anisotropy, dimerization and frustration.

References

[1] White S R and Noack R M 1992 *Phys. Rev. Lett.* **68** 3487
    White S R 1992 *Phys. Rev. Lett.* **69** 2863; 1993 *Phys. Rev.* B **48** 10345
[2] White S R and Huse D A 1993 *Phys. Rev.* B **48** 3844
    Sørensen E S and Affleck I 1993 *Phys. Rev. Lett.* **71** 1633
    Bursill R J, Xiang T and Gehring G A 1994 *J. Phys. A: Math. Gen.* **28** 2109
    Bursill R J, Gehring G A, Farnell D J J, Parkinson J B, Tao Xiang and Chen Zeng 1995 *J. Phys. C: Solid State Phys.* **7** 8605
    White S R, Noack R M and Scalapino D J 1994 *Phys. Rev. Lett.* **73** 886
    Noack R M, White S R and Scalapino D J 1994 *Phys. Rev. Lett.* **73** 882
    Caron L G and Moukouri S 1996 *Phys. Rev. Lett.* **76** 4050
    Gehring G A, Bursill R J and Xiang T 1996 *Acta Phys. Pol.* at press
[3] Pang H B, Akhlaghpour H and Jarrell M 1996 *Phys. Rev.* B **53** 5086
    Hallberg K A 1995 *Phys. Rev.* B **52** R9827
[4] Liang S and Pang H 1995 *Europhys. Lett.* **32** 173
    Xiang T 1996 *Phys. Rev.* B **53** 10445
    White S R 1996 Spin gaps in a frustrated Heisenberg model for CaV$_4$O$_9$ *Preprint*
    White S R and Scalapino D J 1996 Hole and pair structures in the t–J model *Preprint*
[5] Nishino T 1995 *J. Phys. Soc. Japan* **64** 3598
    Nishino T, Okunishi K and Kikuchi M 1996 *Phys. Lett.* **213A** 69
[6] Bulaevskii L N 1963 *Sov. Phys.–JETP* **17** 1008
[7] Suzuki M and Inoue M 1987 *Prog. Theor. Phys.* **78** 787
    Inoue M and Suzuki M 1988 *Prog. Theor. Phys.* **79** 645